Photosensitivity Analysis of Low-Temperature Poly-Si Thin-Film Transistor Based on the Unit-Lux-Current

Ya-Hsiang Tai, Yan-Fu Kuo, and Yun-Hsiang Lee

***Abstract*—In this paper, the photosensitive effect of n-type low-temperature polycrystalline-silicon thin-film transistors (TFTs) is investigated. A novel layout is adopted to demonstrate that the photo leakage current occurs in the depletion region at the drain junction. Based on the Poole–Frenkel effect lowering of a coulombic barrier and phonon-assisted tunneling, it is discovered that the photosensitivity behavior for poly-Si TFT is dependent on the gate and drain bias. However, this photoinduced leakage current behavior is not included in the present SPICE device model. Therefore, a new parameter, unit-lux-current (ULC), is proposed to depict the photoinduced current. Its dependence on the gate/drain bias and temperature is discussed, and the equation of ULC is further derived, which has good agreement with the experimental data. A qualitative deduction is developed to account for the photo leakage mechanism. ULC variation with respect to defect states in the drain region is also discussed.**

***Index Terms*—Leakage current, photo sensitivity, poly-Si thin-film transistor (TFT).**

I. Introduction

LOW-TEMPERATURE polycrystalline-silicon (LTPS) thin-film transistors (TFTs) have attracted much attention for active-matrix liquid crystal display and active-matrix organic light-emitting diode applications due to the high mobility and the capability of realizing integrated circuits on glass. It could reduce the difficulties of the connection of the surrounding circuits and the cost of the panel [1]. The photosensitivity of LTPS TFTs is a significant design consideration for achieving high-image-quality display panels since it will affect the leakage current. Furthermore, several ambient light sensors using the off current of LTPS TFTs have been reported [2]–[7]. Thus, the photosensitive behavior of LTPS TFT off current is of great interest. In this paper, a new parameter is used to analyze the effects of illumination on LTPS TFTs.

Manuscript received July 8, 2008; revised October 16, 2008. Current version published December 19, 2008. This work was supported in part by the National Science Council, China under Grant NSC 97-2218-E-009-005 and in part by MOE ATE Program and MOEA Technology Development Academia Project 96-EC-17-A-07-S1-046. The review of this paper was arranged by Editor L. Lunardi.

Y.-H. Tai and Y.-H. Lee are with the Department of Photonics and the Display Institute, National Chiao Tung University, Hsinchu 30010, Taiwan (e-mail: yhtai@mail.nctu.edu.tw).

Y.-F. Kuo is with the Department of Photonics and the Institute of Electro-Optical Engineering, National Chiao Tung University, Hsinchu 30010, Taiwan.

Color versions of one or more of the figures in this paper are available online at http://ieeexplore.ieee.org.

Digital Object Identifier 10.1109/TED.2008.2009026

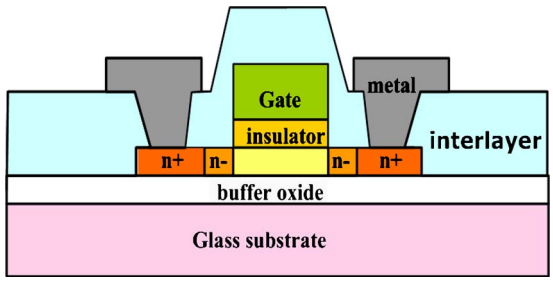

Fig. 1. Cross-sectional views of n-channel LTPS TFTs with LDD structure.

An equation is provided to properly describe ULC under various bias and temperature conditions for further exploration of photo leakage mechanism. In addition, since LTPS TFTs suffer from huge variation owing to the diverse and complicated grain distribution in the poly-Si film [8], ULC variation will also be discussed.

II. Experiments

The self-aligned structure of top-gate n-type LTPS TFTs with lightly doped drain (LDD) structure was used in the experiment. First, the buffer oxide and a-Si:H films were deposited on glass substrates with PECVD. The samples were then put in the oven for dehydrogenation. Then, the XeCl excimer laser scanned the a-Si:H film to recrystallize the a-Si:H film to poly-Si. After poly-Si active area definition, 65-nm SiO_2 was deposited with PECVD as the gate insulator. Next, the metal gate was formed by sputter and then defined. LDD and the n^+ source/drain doping were formed by PH_3 implantation with dosages of 2×10^{13} and 2×10^{15} cm^{-2}, respectively. The LDD implantation was self-aligned, and the n^+ regions were defined with a separate mask. Then, the interlayer of SiN_x was deposited. Subsequently, rapid thermal annealing was conducted to activate the dopants, while the poly-Si film was simultaneously hydrogenated for 30 min. Finally, contact hole formation and metallization were performed to complete the fabrication work. The cross-sectional view of n-channel LTPS TFTs is shown in Fig. 1. In this paper, the TFTs having a channel width of 20 μm and a channel length of 5 μm with LDD structure of length 2.5 μm are measured under different illumination conditions. The light was collimated and focused onto the device with top-face white-light illumination. Photo leakage current was induced by a halogen lamp irradiation stream with

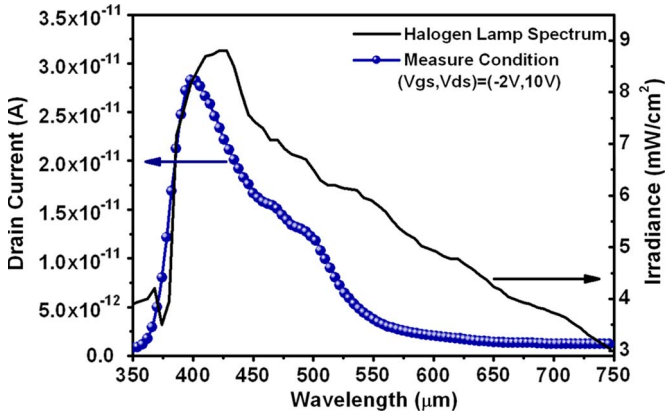

Fig. 2. Photo leakage current and the power variation spectrum of the light source.

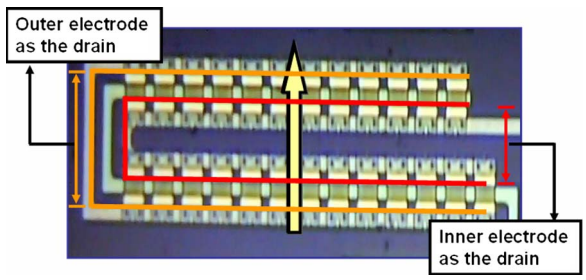

Fig. 3. Photograph of the special U-shaped TFT with an arrow indicating the scanning path of the illumination beam.

several neutral density filters (light intensity ranging from dark to 31 320 lux) through the objective of a microscope, and the light intensity was measured by a digital luminous flux meter.

Fig. 2 shows the photo leakage current and the power variation spectrum of the light source in the range of 350–750 nm. The lower drain current at long wavelengths may be due to photon absorption in the gate and other multilayer structure of the TFT.

III. Results and Discussion

A. Sensing Area Consideration

Before the mechanism of photosensitivity is discussed explicitly, it should be first examined where the most sensitive to the illumination inside LTPS TFTs is. A special layout of the TFT with U-shaped source and drain electrode configuration is adopted in this paper, as shown in Fig. 3. Twenty-five TFTs are arranged in parallel and separated into two groups. The upper group consists of 12 TFTs, and the lower one contains 13 TFTs. The inner electrodes (about 33-μm distance) of the TFTs in these two groups are shorted together and so are the outer electrodes (about 59-μm distance) to form the U-shaped TFT.

An irradiation optical beam with 25-μm light spot radius has been used to directly shine on the device. By scanning the beam along the channel direction of the U-shaped TFT, the leakage currents of the LTPS TFT are measured in two cases with the inner or the outer electrodes as drain. As shown in

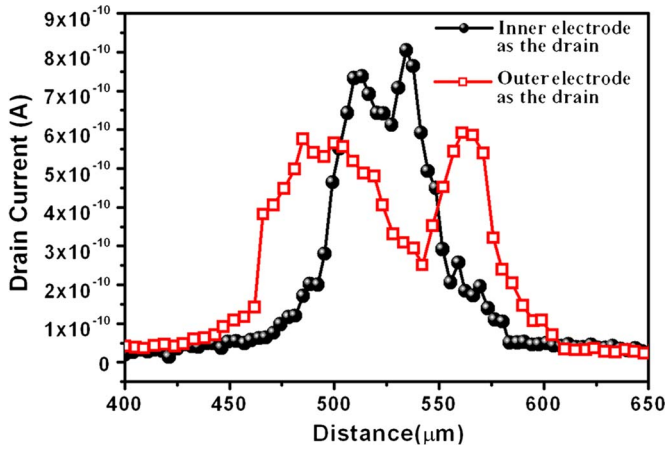

Fig. 4. Drain current of the U-shaped TFT with the distance of the illumination beam scanned along the channel direction.

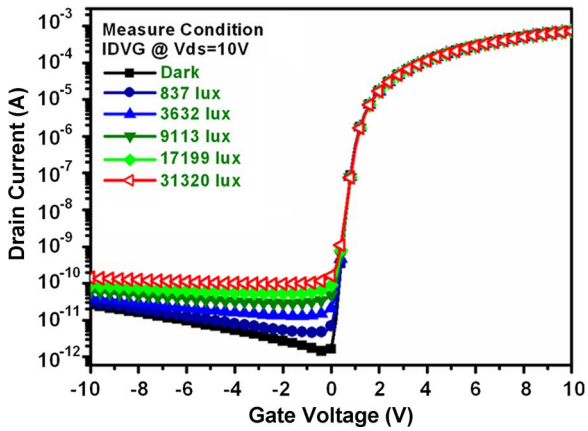

Fig. 5. I_D–V_G transfer characteristics under illumination from dark to 31 320 lux.

Fig. 4, two anomalous peaks of the off current are observed. When the measurement is performed with outer electrodes as drain, the distance is larger (about 66 μm). On the other hand, when the inner electrodes are used as the drain, the distance is shorter (about 32 μm). The distance between the pair peaks is consistent with the device's real junction distance. It reveals that the photoinduced current happens only at the drain side. Therefore, the following discussion of the photosensitivity mechanism will focus only on the drain region.

B. Definition of the Index for Photosensitivity and Analysis

The typical I_D–V_G transfer characteristics of the LTPS TFT under illumination from dark to 31 320 lux are shown in Fig. 5. It can be seen that the off current increases with the intensity of the incident light, and it has weak gate bias dependence under higher ambient light intensity. There are several parameters that can be used to describe this behavior of the photoinduced off current. To discuss the photo effect of TFTs, the previous study [9] used an index $R_{L/D}$ defined as the ratio of the current under illumination (I_{total}) to the current in the dark (I_{Dark}). $R_{L/D}$ is suitable to evaluate the performance of light sensors. However, it may not be proper to be used to analyze photo leakage

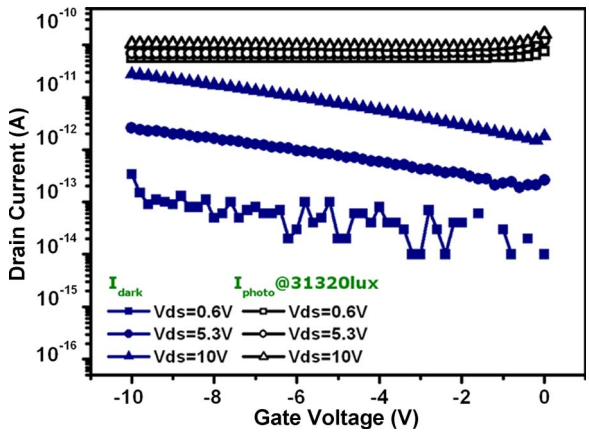

Fig. 6. Gate bias dependence of LTPS TFT photo currents and dark currents in the off region.

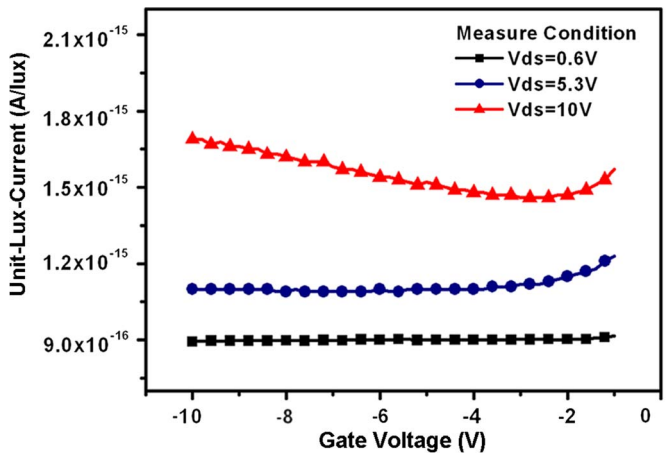

Fig. 8. Gate bias effect on ULC at different drain biases.

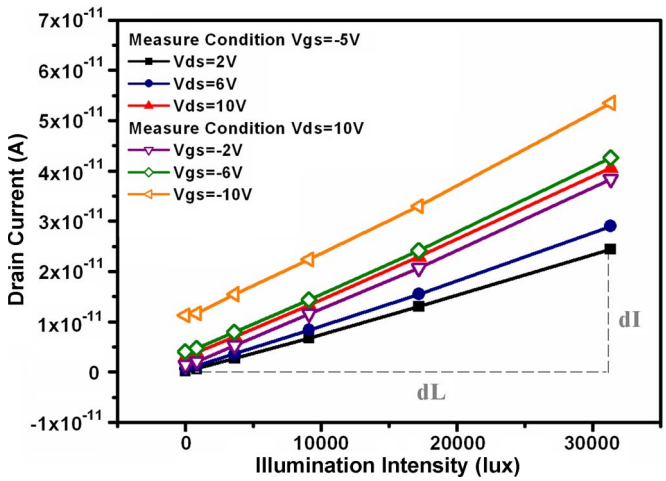

Fig. 7. Relationship between leakage current and illumination intensity under different bias conditions.

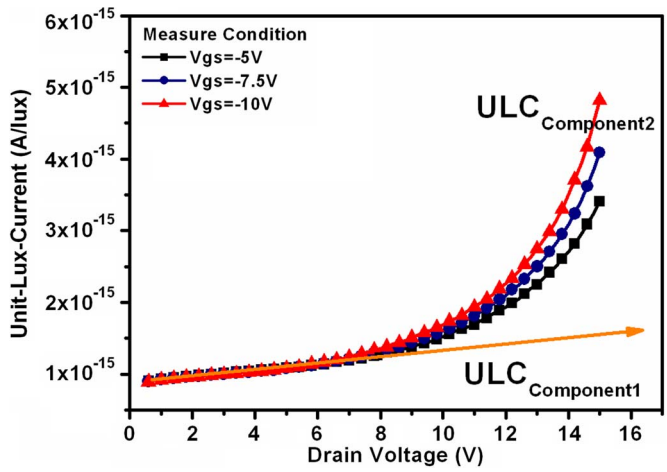

Fig. 9. Drain bias effect on ULC at different gate biases.

mechanism. As shown in Fig. 6, because $I_{\rm total}$ is less dependent on the gate voltage, $R_{L/D}$ is mostly determined by the behavior of $I_{\rm Dark}$. It cannot reflect photo behaviors of TFTs. Therefore, for our discussion, it may be necessary to find another index which can eliminate the influence of $I_{\rm Dark}$.

Fig. 7 shows the relationships between drain current and illumination intensity for several bias conditions in the off region. It can be seen that all drain currents are proportional to the amount of radiant illumination. Thus, it can be taken that the total leakage current under illumination $(I_{\rm total})$ is composed of two components: One is the leakage current that is not caused by photo illumination $(I_{\rm Dark})$ which is measured under dark state. In addition, the other part is illumination-induced leakage current $(I_{\rm Illum})$ which denotes the component induced by illumination. In this paper, we will offset $I_{\rm Dark}$ and only consider $I_{\rm Illum}$ which is defined to be the difference between $I_{\rm total}$ and $I_{\rm Dark}$. To analyze the photosensitivity of LTPS TFTs in detail, we further define the slope of the curve in which the current versus illumination intensity corresponds to the unit-lux-current (ULC) that is considered a new index. The physical meaning of ULC is the photo leakage current induced "per unit-photo flux" and independent of the dark current. Therewith, the total off current $I_{\rm total}$ of LTPS TFT can be expressed as

$$I_{\rm total} = I_{\rm Dark} + I_{\rm Illum} = I_{\rm Dark} + {\rm ULC} \cdot L \qquad (1)$$

where L is the illumination intensity in lux.

C. Field Effects on ULC

Fig. 8 shows the gate bias dependence of ULC under different drain biases. It is obvious that ULC is changed severely under higher drain voltage. Fig. 9 shows the drain bias dependence of ULC under different gate biases. When drain voltage Vd is lower than 8 V, ULC increases linearly with drain bias [10], and gate bias effect is negligible. However, when Vd is large enough, ULC increases with drain bias more rapidly, and gate bias effect becomes significant. As shown by the arrow line in Fig. 9, the linear ULC curve at low drain bias can be fit, and this is one of the two components of the total ULC. This component which increases with drain bias linearly and independent of gate bias is defined as $\rm ULC_1$. Then, the second component which subtracts $\rm ULC_1$ from the total ULC curve is called $\rm ULC_2$.

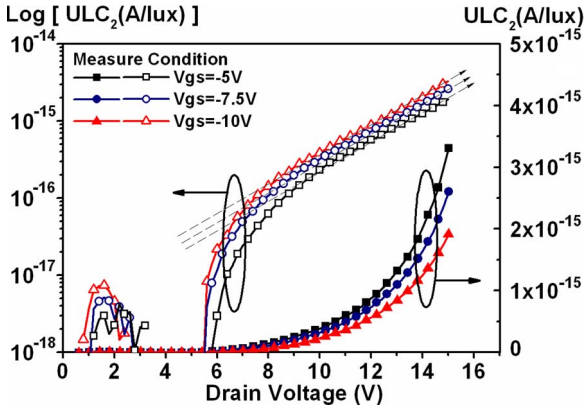

Fig. 10. Second component of ULC (ULC_2) versus drain bias at different gate voltages.

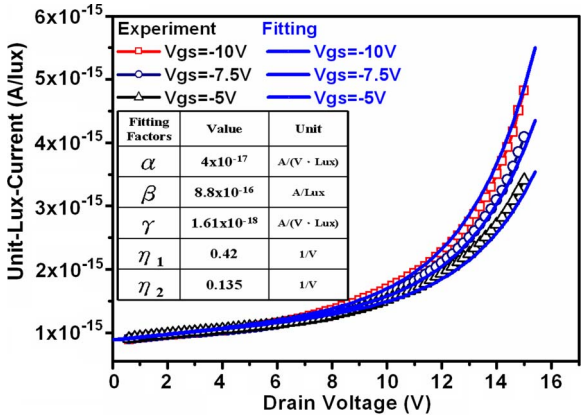

Fig. 11. Calculated and experimental data of drain bias effect on ULC at different gate biases.

Furthermore, we show ULC_2 in Fig. 10. It is apparent that the log $[\mathrm{ULC}_2]$ increases with drain bias linearly, indicating that ULC_2 increases with drain bias exponentially when Vd is large enough. The parallel curves of log $[\mathrm{ULC}_2]$ at different gate biases indicate that the dependence of gate bias is also exponential. Thus, ULC can be expressed by a linear combination of these two components as

$$\mathrm{ULC} = \mathrm{ULC}_1 + \mathrm{ULC}_2 \tag{2}$$

$$\mathrm{ULC}_1 = \alpha \mathrm{Vd} + \beta \tag{3}$$

$$\mathrm{ULC}_2 = \gamma \cdot \exp(\eta_1 \mathrm{Vd} - \eta_2 \mathrm{Vg}) \tag{4}$$

where α, β, γ, η_1, and η_2 are all fitting parameters. α and β correspond to the linear drain voltage dependence and the zero drain bias offset of ULC_1, respectively. γ is the scaling factor of ULC_2, while η_1 and η_2 are the parameters about the exponential dependence on the drain bias and negative gate bias of ULC_2, respectively. As shown in Fig. 11, the calculated results agree with our experiment data very well. The values of fitting parameters are also listed in the inset.

Moreover, the mechanisms of two ULC components will be further discussed. The ULC can be taken into account as the leakage current induced both in the gate–drain overlap depletion and lateral depletion regions [11]. When the device is operating at low drain voltage, the linear increase with

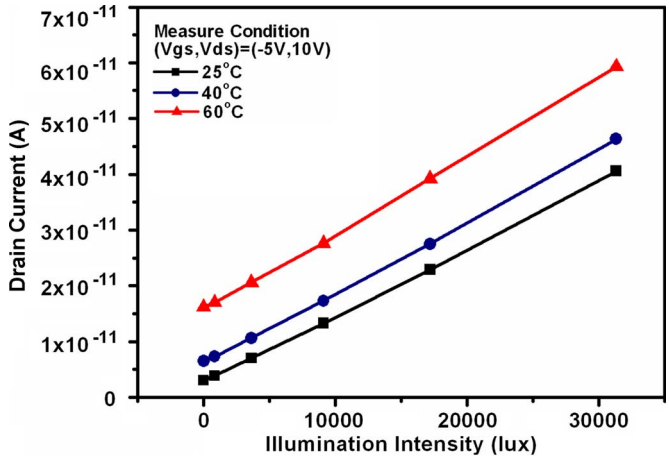

Fig. 12. Temperature effect on photo leakage current of LTPS TFT.

the drain bias of ULC_1 is attributed to the lateral depletion region by the channel–drain junction in reverse bias. In this region, ULC_2 is negligible. When drain voltage is large enough, ULC_2 increases with drain exponentially, and gate bias effect becomes significant. Several mechanisms of leakage current were discussed in previous reports [12]–[15]. It is considered that the reverse lateral depletion at the drain region extends and causes gate-induced drain leakage (GIDL) in the gate–drain overlap depletion junction. The amount of photo current should be associated with the carrier generation in the space-charge region. By the junction reverse saturation current and GIDL, the drain current owing to the GIDL effect is also in an exponential relation. This phenomenon is similar to our case of ULC_2 component. The voltage difference between the drain and gate biases corresponds to the magnitude of electric field across the depletion region. A more negative gate bias means that the electric field would get stronger (the same as a more positive drain bias). It suggests that larger electric field across the drain depletion region causes larger photo effect. Both drain and gate bias affect the electric field strength in the depletion region in slightly different ways.

D. Temperature Effects on ULC

We further take into account temperature effects on ULC. Fig. 12 shows the illumination effect on photo leakage current at different temperatures of 25, 40, and 60 °C under a certain bias condition of $(\mathrm{Vd}, \mathrm{Vg}) = (10\ \mathrm{V}, -5\ \mathrm{V})$. The correlation between I_{total} and illumination intensity is still linear at various temperatures.

Drain bias dependences of ULC at different temperatures are shown in Fig. 13. The ULC in the range of low drain bias is significantly affected by temperature, while that in the higher drain bias range is gradually and less affected by temperature. From the discussion earlier, we have separated the ULC into ULC_1 and ULC_2. It can be seen that ULC_1 is actually the term subject to the temperature effect. On the other hand, as shown in Fig. 14, ULC_2 is totally temperature independent, which means that ULC_2 is the term purely induced by electric field. Therefore, ULC_1 may be induced by mechanism like excess carrier diffusion or thermionic emission, and thus, it has weak

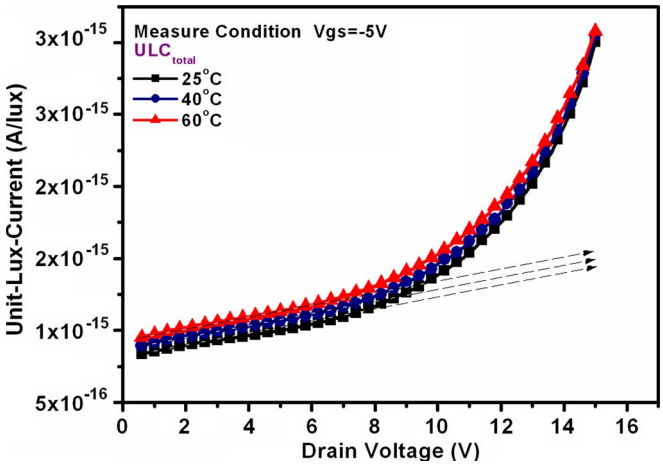

Fig. 13. Drain bias dependence of ULC at different temperatures.

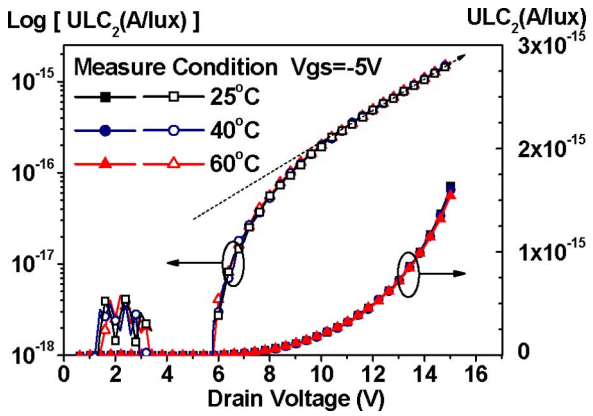

Fig. 14. Second component of ULC (ULC_2) versus drain bias with different temperatures.

dependence on the electric field, particularly on the gate bias. ULC_2 may be induced by mechanism like excess carrier drift or field emission, and thus, it has strong dependence on the drain and gate biases.

Since the lateral electric field is relatively small, the photo-induced current is a thermally generated current dominantly. The temperature effect on I_{Dark} can identify constant activation energy [16], [17], which hints us to add the fitting factors α and β in (4) in the Arrhenius plot. Fig. 15 shows the relationship between α and β and $1/kT$. These two factors increase with $1/kT$ exponentially and can be expressed by

$$\alpha = A \cdot \exp(-Ea_A/kT) \tag{5}$$

$$\beta = B \cdot \exp(-Ea_B/kT) \tag{6}$$

where Ea_A and Ea_B are the activation energies of α and β, respectively, and A and B are their corresponding fitting parameters. The fitting values of Ea_A, Ea_B, A, and B are listed in the inset. By the temperature effect discussed previously, it is confirmative to separate ULC into two components. ULC_1 is thermally activated and might be corresponding to thermionic emission or carrier diffusion, while ULC_2 is independent of temperature and possibly owing to field emission or carrier drift.

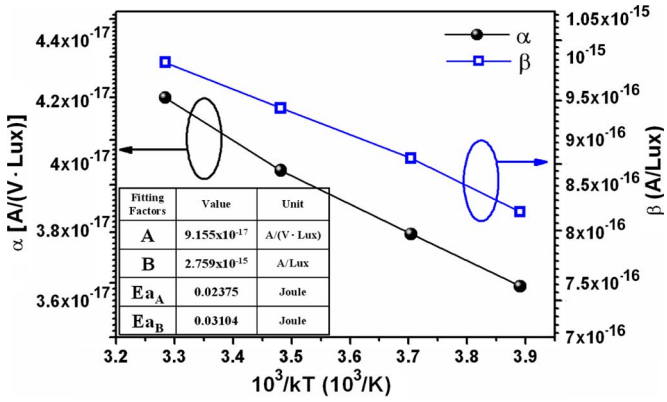

Fig. 15. Dependence of factors α and β on temperature.

E. Mechanism of ULC

Based on the experimental results of bias, temperature, and sensing location, a more complete mechanism of ULC is proposed to explain the photosensitive effect on the leakage current of LTPS TFT. Fig. 16 shows the band diagrams under the condition of $\mathrm{Vg} < 0$ along the channel direction near the drain region at low and high drain biases. In the figure, Wd indicates the length of the depletion region at the drain electrode side where electron–hole pairs can be generated under illumination in the poly-Si film. The generated electrons flow toward the drain electrode, and the holes flow in the opposite direction. Wd consists of two regions. One is the high-hole-concentration region in the channel induced by the negative gate bias, and the other is in the LDD region. The channel area is shielded by the gate metal, while the LDD region can be shined by the illumination. Based on the Poole–Frenkel effect lowering of a coulombic barrier and phonon-assisted tunneling due to the electric field applied to a semiconductor [18], which enhances thermal emission and the trap-to-band field emission rate, the two components of ULC will be discussed. For the case at low drain bias with light irradiation, when the gate bias is changed, similarly to the abrupt $\mathrm{p}^+\mathrm{n}$ junction, the electric field of the other part in the LDD region is invariable. Thus, the gate voltage independence of ULC_1 can be explained. As for the Vd effect, the lateral depletion region increases linearly with drain bias, corresponding to the parameter α in (3). With extremely low drain bias, there is still a depletion region in LDD, in accordance with the parameter β in (3). The conduction mechanism of the leakage current in the low drain field is thermal emission [19]. Consequently, the parameters α and β of ULC_1 are temperature dependent.

On the other hand, for the high drain bias with light irradiation, the electric field across the lateral depletion region is large enough to fully deplete the LDD region. Therefore, the increase of drain voltage will increase the electric field within the limited LDD length pinched by the n^+ region. In such a case, the more negative gate bias will also result in a larger field with the same depletion width of the LDD region. The conduction mechanism of the leakage current at the high drain voltage is field-enhanced emission in the space-charge region [20]. The electric field dependence of ULC_2 is reflected by the slightly different values of the fitting parameters η_1 and η_2 in (4).

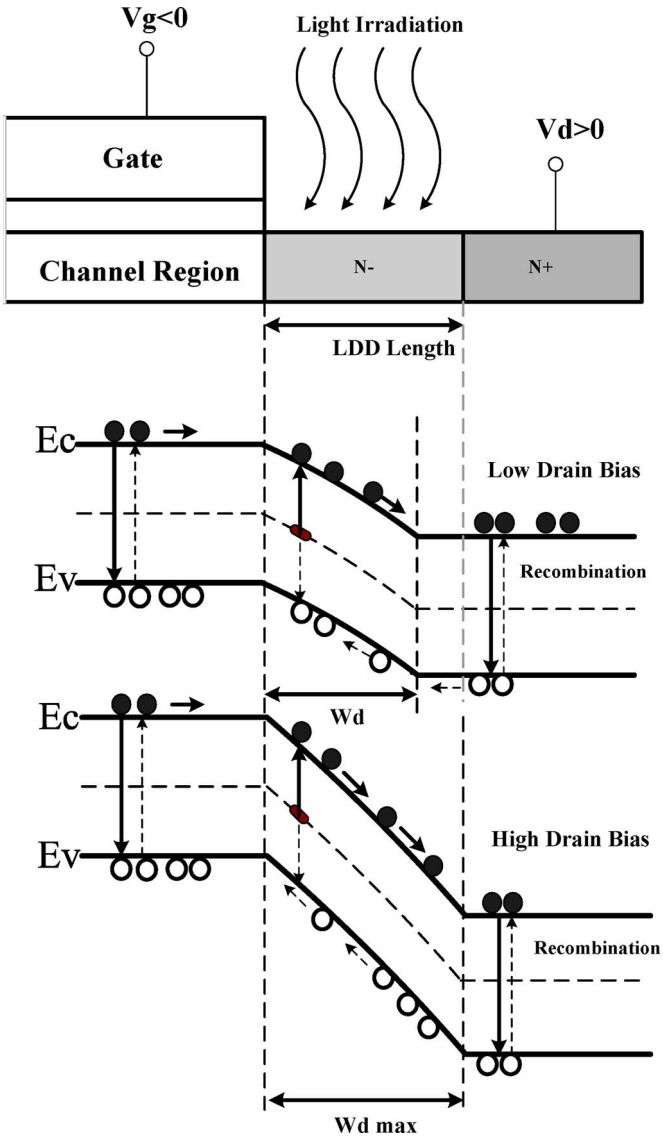

Fig. 16. Proposed model of ULC mechanism for LTPS TFTs.

F. Devices Variation

The uniformity of LTPS TFT is always an important issue. Different devices even fabricated by the same process suffer from serious device variation, particularly for the off current. For this consideration, photo leakage currents would also vary among devices. Fig. 17 shows photo leakage currents with respect to the illumination intensity of several devices on the same glass. It verifies that there is still serious device variation in the aspect of photo leakage current. The results further confirm that the mechanisms of the photosensitivity for the LTPS TFT are closely related to the different defect distribution or density in the grain boundary, alike the case of the dark off current. This issue needs to be overcome before LTPS TFTs can be practically used as photo-sensing devices.

IV. Conclusion

In this paper, we present detail studies on the factors that affect the photo leakage current like bias condition, temperature, and defect states of LTPS TFTs. It is found that the photo leakage current always exhibits good linear dependence on illumination intensity. Thus, a new index ULC characterizing the slope of the curve is introduced to discuss the photosensitivity. Furthermore, the mechanism of the photosensitivity for LTPS TFTs is proposed. It relates to the width and electric field in the lateral depletion region near the drain. It is also shown that ULC variation is also related to defects in the depletion region. The empirical equation of ULC provides a potential modeling for simulation of LTPS TFT circuitry considering the photo effect.

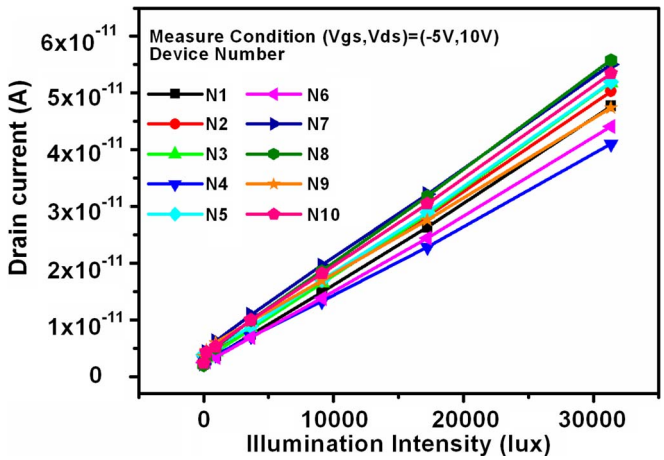

Fig. 17. Photo leakage current variation among different devices.

References

[1] Y. H. Tai, C. C. Pai, B. T. Chen, and H. C. Cheng, "A source-follower type analog buffer using poly-Si TFTs with large design windows," *Electron. Lett.*, vol. 26, no. 11, pp. 813–881, Nov. 2005.

[2] F. Matsuki, K. Hashimoto, K. Sano, D. Yeates, J. R. Ayres, M. Edwards, and A. Steer, "Integrated ambient light sensor in LTPS AMLCDs," in *Proc. Soc. Inf. Display*, 2007, pp. 290–293.

[3] H. S. Lim and O. K. Kwon, "Ambient light sensing circuit using LTPS TFTs for auto brightness control," in *Proc. Dig. Tech. Workshop Active-Matrix Flat Panel Displays Devices*, 2006, pp. 21–24.

[4] S. Koide, S. Fujita, T. Ito, S. Fujikawa, and T. Matsumoto, "LTPS ambient light sensor with temperature compensation," in *Proc. Int. Display Workshop*, 2006, pp. 689–690.

[5] M. Inoue and H. Ohshima, "LTPS technologies for advanced mobile display applications," in *Proc. Dig. Tech. Workshop Active-Matrix Flat Panel Displays*, 2007, pp. 215–219.

[6] C. Brown, H. Kato, K. Maeda, and B. Hadwen, "A CG silicon system LCD with optical input function," in *Proc. Int. Display Workshop*, 2000, pp. 99–103.

[7] T. Eguchi, Y. Hiyoshi, E. Kanda, H. Sera, T. Ozawa, T. Miyazawa, and T. Matsumoto, "A 1300-dpi optical image sensor using an a-Si:H photo diode array driven by LTPS TFTs," in *Proc. Soc. Inf. Display*, 2007, pp. 1097–1100.

[8] W. Albert and W. Saraswat, "Strategy for modeling of variations due to grain size in polycrystalline thin-film transistors," *IEEE Trans. Electron Devices*, vol. 47, no. 5, pp. 1035–1043, May 2000.

[9] J.-D. Gallezot, M. Sandrine, and K. Jerzy, "Photosensitivity of a-Si:H TFTs," in *Proc. SID Conf. Rec. Int. Display Res. Conf.*, 2001, pp. 407–410.

[10] T. Yamashita, T. Shima, Y. Nishizaki, M. Kimura, H. Hara, and S. Inoue, "Evaluation of thin-film photodiodes and development of thin-film phototransistor," *Jpn. J. Appl. Phys.*, vol. 47, no. 3, pp. 1924–1929, Mar. 2008.

[11] W. J. Wu, R. H. Yao, S. H. Li, Y. F. Hu, W. L. Deng, and X. R. Zheng, "A compact model for polysilicon TFTs leakage current including the Poole–Frenkel effect," *IEEE Trans. Electron Devices*, vol. 54, no. 11, pp. 2975–2983, Nov. 2007.

[12] J. H. Chen, S. C. Wong, and Y. H. Wang, "An analytic three-terminal band-to-band tunneling model on GIDL in MOSFET," *IEEE Trans. Electron Devices*, vol. 48, no. 7, pp. 1400–1453, Jul. 2001.

[13] C. S. Chuang, T. C. Fung, B. G. Mullins, J. Kanicki, K. Nomura, T. Kamiya, H. Hosono, and H. P. Shieh, "Photosensitivity of amorphous IGZO TFTs for active-matrix flat-panel displays," in *Proc. Soc. Inf. Display*, 2008, pp. 1215–1218.
[14] J. R. Ayres, S. D. Brotherton, I. R. Clarence, and P. J. Dobson, "Photocurrents in poly-Si TFTs," *Proc. Inst. Elect. Eng.—Circuits, Devices Syst.*, vol. 141, no. 1, pp. 27–32, Feb. 1994.
[15] N. P. Papadopoulos, A. A. Hatzopoulos, D. K. Papakostas, C. A. Dimitriadis, and S. Siskos, "Modeling the impact of light on the performance of polycrystalline thin-film transistors at the sub-threshold region," *Microelectron. J.*, vol. 37, no. 11, pp. 1313–1320, Nov. 2006.
[16] A. Pecora, M. Schillizzi, G. Tallarida, G. Fortunato, C. Reita, and P. Migliorato, "Off-current in polycrystalline silicon thin film transistors: An analysis of the thermally generated component," *Solid State Electron.*, vol. 38, no. 4, pp. 845–850, Apr. 1995.
[17] O. Kikuo, A. Takashi, K. Nobutake, and M. Kenji, "Analysis of current voltage characteristics of low-temperature-processed polysilicon thin-film transistors," *IEEE Trans. Electron Devices*, vol. 39, no. 4, pp. 792–802, Apr. 1992.
[18] O. K. B. Lui and P. Migliorato, "New generation–recombination model for device simulation including the Poole–Frenkel effect and phonon-assisted tunnelling," *Solid State Electron.*, vol. 41, no. 4, pp. 575–583, Apr. 1997.
[19] C. H. Kim, K.-S. Sohn, and J. Jang, "Temperature dependent leakage currents in polycrystalline silicon thin film transistors," *J. Appl. Phys.*, vol. 81, no. 12, pp. 8084–8090, Jun. 1997.
[20] G. Fortunato and P. Migliorato, "Determination of gap state density in polycrystalline silicon by field-effect conductance," *Appl. Phys. Lett.*, vol. 49, no. 16, pp. 1025–1027, Oct. 1986.

Ya-Hsiang Tai received the B.S. and Ph.D. degrees in electronic engineering from National Chiao Tung University, Hsinchu, Taiwan, in 1990 and 1996, respectively.

He joined the project of low-temperature polycrystalline silicon (LTPS) thin-film transistor (TFT) development in Prime View International Company Limited, in 2000. In 2001, he was with Toppoly Optoelectronics Corporation to lead the team of LTPS TFT LCD panel design. He has been a Faculty Member at National Chiao Tung University since 2003, where he is currently an Assistant Professor with the Department of Photonics and the Display Institute. His current research emphases include TFT device physics, active matrix display panel design, and system on panel.

Dr. Tai is a member of Phi Tau Phi. He was a member of Industrial Technology Research Institute/Electronics Research & Service Organization and became part of the TFT LCD development as a Panel Designer.

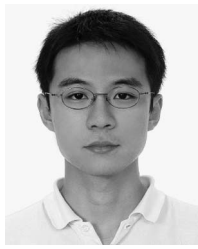

Yan-Fu Kuo received the B.S. degree in physics from National Sun Yat-Sen University, Kaohsiung, Taiwan, in 2002 and the M.S. degree in electro-optical engineering from National Chiao Tung University, Hsinchu, Taiwan, in 2004, where he is currently working toward the Ph.D. degree.

He is currently with the Department of Photonics and the Institute of Electro-Optical Engineering, National Chiao Tung University. His current research interests include sensors and applications of low-temperature poly-Si TFTs.

Yun-Hsiang Lee received the B.S. degree in physics from National Cheng Kung University, Tainan, Taiwan, in 2006.

He is currently with the Department of Photonics and the Display Institute, National Chiao Tung University, Hsinchu, Taiwan. His current research interest includes light-sensing functions of low-temperature poly-Si TFTs.